



Note

Conformational studies of the capsular polysaccharide produced by *Neisseria meningitidis* group A

Michela Foschiatti^a, Meredith Hearshaw^b, Paola Cescutti^a, Neil Ravenscroft^b, R. Rizzo^{a,*}

^a Department of Life Sciences, University of Trieste, Bldg C11, Via Licio Giorgieri 1, 34127 Trieste, Italy

^b Department of Chemistry, University of Cape Town, Rondebosch, 7701, South Africa

ARTICLE INFO

Article history:

Received 16 December 2008

Received in revised form 19 February 2009

Accepted 20 February 2009

Available online 4 March 2009

Keywords:

Neisseria meningitidis

Capsular polysaccharide

Structure

Conformation

Atomic force microscopy

Vaccines

ABSTRACT

The effect of different cations on the conformational and morphological properties of the capsular polysaccharide produced by *Neisseria meningitidis* group A was investigated. Circular dichroism studies showed that the presence of Na⁺, NH₄⁺ or Ca²⁺ ions induced different local conformations of the polysaccharide chain through interactions with the phosphodiester group bridging the saccharide residues in the polymer chain. Atomic force microscopy experiments confirmed that the morphology of the polysaccharide chains was different depending on the nature of the counterion. Ammonium ions were associated with the presence of single polymer chains in an elongated conformation, whereas sodium ions favored the folding of the chains into a globular conformation. The addition of calcium ions produced the aggregation of a limited number of globular polysaccharide chains to form a 'toroidal-like' structure.

© 2009 Elsevier Ltd. All rights reserved.

The highest burden of meningococcal disease occurs in the 'Meningitis Belt' in sub-Saharan Africa, a region characterized by high levels of endemic meningococcal disease and large epidemics that occur in the dry season, periodically every 2–10 years.¹ In 1996, Africa experienced the largest recorded outbreak of epidemic meningitis in history, with over 250,000 cases and 25,000 deaths registered. *Neisseria meningitidis* group A accounts for about 80–85% of all cases. Epidemics are controlled by mass immunization campaigns with meningococcal polysaccharide vaccines that are of limited effectiveness and do not induce herd immunity. Conjugate vaccines are immunogenic in the very young, induce immunological memory and are likely to give long-lasting protection and thus provide an opportunity to eliminate meningococcal epidemics. The Meningitis Vaccine Project (MVP) is a partnership between WHO and the non-governmental organization Program for Appropriate Technology in Health (PATH), which was established in 2001. MVP has the goal of eliminating epidemic meningitis through the development and widespread introduction of an affordable group A meningococcal conjugate vaccine.² Clinical trials have shown the vaccine to be safe and highly immunogenic

with serum bactericidal titers 20 times higher when compared to polysaccharide vaccine.³

The conjugate vaccine consists of *N. meningitidis* group A polysaccharide (partly O-acetylated α -(1→6)-linked *N*-acetylmannosamine phosphate) that is activated by periodate oxidation and conjugated to hydrazide-derivatized tetanus toxoid (TT) as carrier protein.⁴ Periodate treatment then oxidizes some of the non-O-acetylated residues present (5–10%) to generate aldehyde groups at C3 and C4 of those residues, which are then used for conjugation. During development of the vaccine, three lots of polysaccharides prepared using a modified purification process proved to be resistant to periodate oxidation. These lots were of similar molecular weight and degree of O-acetylation to previous lots, the only difference was in the calcium/phosphorus ratio, which was assumed to have resulted in a divalent-cation/polysaccharide interaction leading to a conformation that prevented periodate oxidation. It is worth noting that high calcium ions concentration result in precipitation of the *N. meningitidis* polysaccharide (Mn A). These observations prompted the present study to investigate the effect of counterions on the conformation of this polysaccharide.

Mn A is a polyelectrolyte whose repeating unit structure is shown in Figure 1, where the conformational degrees of freedom are indicated by arrows. Acetyl groups are present on 85–90% of the repeating units on the ring carbons. The polymer bears one net negative charge for every saccharide repeating unit due to the presence of a phosphodiester glycosidic bond. The presence

Abbreviations: AFM, atomic force microscopy; CD, circular dichroism; MVP, Meningitis Vaccine Project; Mn A, *Neisseria meningitidis* polysaccharide; PATH, Program for Appropriate Technology in Health; TT, tetanus toxoid.

* Corresponding author. Fax: +39 040 676 3691.

E-mail address: rizzor@units.it (R. Rizzo).

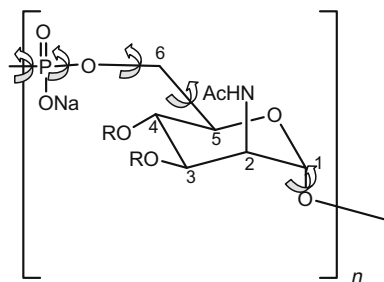


Figure 1. Mn A repeating unit $[-\rightarrow 6)-\alpha\text{-D-ManpNAC}(3/4\text{OAc})-(1\rightarrow\text{OPO}_3\rightarrow)_n$. The conformational degrees of freedom are represented by arrows. R are acetyl groups.

of the phosphodiester bond and the (1 \rightarrow 6) inter-residue linkage suggests high flexibility of the polymer chain conformation. In fact, the polymer contains two more rotational degrees of freedom with respect to those exhibited by a conventional (1 \rightarrow 6) O-glycosidic bond (Fig. 1). However, due to its polyelectrolyte character, the overall conformation of the polymer chain depends on the concentration of ionic species present in solution. On one hand, these species affect the solution dielectric constant (ionic strength effect) by lowering attractions and/or repulsions between electric charges. On the other hand, they can specifically interact with the polyelectrolyte chain possibly producing conformational constraints. Some ionic polysaccharides are known to interact with mono- and divalent cations to form aggregates that may result in gel formation. This is the case for algal polysaccharides, like the carrageenans interacting with monovalent cations and alginate interacting with Ca^{2+} ions.^{5,6} Also, bacterial polysaccharides, such as gellan gum produced by *Sphingomonas elodea*, are able to form gels whose texture and quality depend on the concentration of the divalent cations present.⁷

A general pre-requisite of ion-driven ionic polysaccharides association is the formation of regions of secondary structures having variable length, as reported in the gel formation models of carrageenans and alginate. The investigation of the conformational properties of Mn A was based upon these considerations.

Light scattering experiments (Fig. 2), carried out by means of a spectrofluorimeter, indicated that the addition of calcium ions to a solution of Mn A in the sodium form induced a change in the scattered light intensity at a $[\text{Ca}^{2+}]$ to polymer concentration ratio (R) near 0.75, where the polymer concentration was expressed as concentration of repeating unit. The increase of the scattered light intensity upon the addition of Ca^{2+} ions suggested the formation

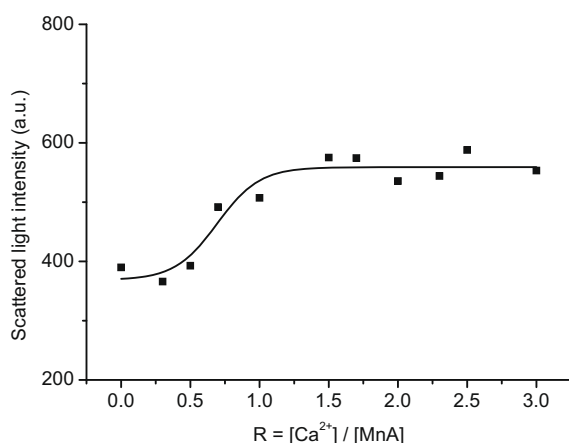


Figure 2. Light scattering data of the addition of Ca^{2+} ions to a Mn A Na^+ solution. $[\text{Mn A}] = 5.7 \times 10^{-3}$ N in the presence of 50 mM NaCl added salt.

of a second species in solution, probably resulting from polymer aggregation. The possibility of inducing Mn A aggregation driven by cations prompted us to investigate this system by use of circular dichroism (CD) which can detect changes in local chain conformations. The presence of acetyl groups bound to the chiral saccharide residue, and absorbing in the 190–230 nm UV region allowed their use as conformational probes. Sodium and ammonium salts of Mn A were used to investigate the effect of the addition of calcium ions to different monovalent cation salt forms of Mn A. Previous studies have shown that ammonium ions can lower the aggregation ability of ionic polysaccharides, thus the comparison of the two salt forms might give additional information about the solution properties of Mn A.^{8,9}

CD data obtained as a function of Ca^{2+} ion addition to Mn A either in the Na^+ form or in the NH_4^+ form are shown in Figure 3. The data of both experiments showed a sigmoidal trend in good agreement with light scattering experiments. Following Ca^{2+} addition, the highest variation of the molar ellipticity was obtained in the $[\text{Ca}^{2+}]/[\text{Mn A}]$ concentration ratio range 0.6–0.7 for both sodium and ammonium salt forms. However, although the molar ellipticity values were very similar at high $[\text{Ca}^{2+}]/[\text{Mn A}]$ concentration ratios, dichroic effects at $[\text{Ca}^{2+}]/[\text{Mn A}] = 0$ were markedly different for the two salt forms. The initial molar ellipticity for the Na^+ salt was about $1700 \text{ deg cm}^2 \text{ dmol}^{-1}$ while that for the NH_4^+ form was about $7700 \text{ deg cm}^2 \text{ dmol}^{-1}$. These findings suggested that the average local conformations of Mn A Na^+ were different from those of the NH_4^+ salt form, and that upon Ca^{2+} addition, the polymer conformation evolved toward a common conformational form.

At this stage of the investigation, it was not possible to define the molecular details of the conformations involved in the Mn A structure in the presence of different counterions. To obtain more information on the general shape of the Mn A molecule and/or aggregates, atomic force microscopy (AFM) experiments were performed.

The images obtained for the Na^+ and NH_4^+ salt forms are shown in Figure 4a and b. They show a different morphology for the two forms. While the Na^+ form had a spherical appearance, the NH_4^+ salt form had a more elongated shape. The spherical morphology of the Na^+ form was attributed to two concomitant effects: (i) the flexibility of the polymer chain due to the high number of conformational degrees of freedom (Fig. 1), and (ii) the interaction of Na^+ ions with the charged phosphate groups of the glycosidic bond. As for the NH_4^+ form, a different local interaction of the cations with phosphate groups might explain the difference in polymer

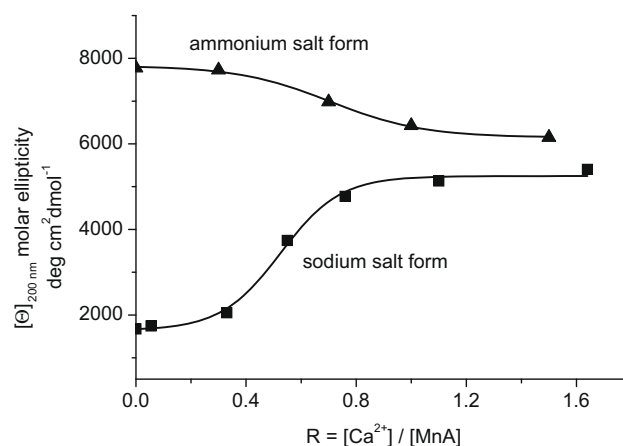


Figure 3. Circular dichroism data of a Mn A solution as a function of the addition of Ca^{2+} ions. (\blacktriangle) Mn A in the NH_4^+ salt form as starting material; (\blacksquare) Mn A in the Na^+ salt form as starting material.

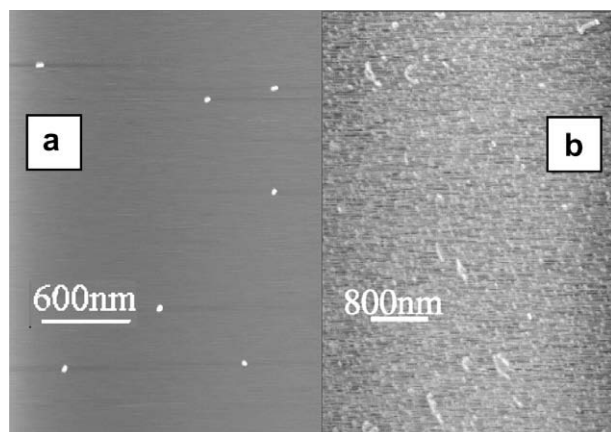


Figure 4. (a) AFM image of the Na^+ salt form of Mn A spray-dried on mica; polymer concentration 5 $\mu\text{g}/\text{mL}$. (b) AFM image of the NH_4^+ salt form of Mn A spray-dried on mica; polymer concentration 5 $\mu\text{g}/\text{mL}$.

morphology; this is also supported by the CD data. It cannot be ruled out that NH_4^+ ions led to a different electrostatic interaction between the negatively charged polymer chain and the mica surface with respect to that mediated by Na^+ ions, thus resulting in a more elongated morphology.¹⁰ However, even in this case, it can be concluded that a different interaction of NH_4^+ and Na^+ ions with the polymer chain was present.

As a control, AFM of dextran, which is a flexible polymer constituted of (1→6)-linked α -glucose, was investigated. The absence of charged groups in dextran makes its average conformation independent of the presence of charged species. An AFM image of dextran is shown in Figure 5. A morphology similar to that of Mn A Na^+ was observed, indicating that, in the absence of electrostatic interactions, the flexibility of the polymer chain played a major role in determining its average shape.

AFM experiments carried out on Mn A Ca^{2+} showed the presence of a macromolecular species with a morphology different from those of both the Na^+ and NH_4^+ forms, again in good agreement with the CD data. An AFM image of Mn A Ca^{2+} deposited onto a freshly cleaved mica surface is shown in Figure 6. The image shows a clear association of spherical particles. It appears that the double charge of calcium ions produced a number of interactions between segments of the polymer chain as well as between

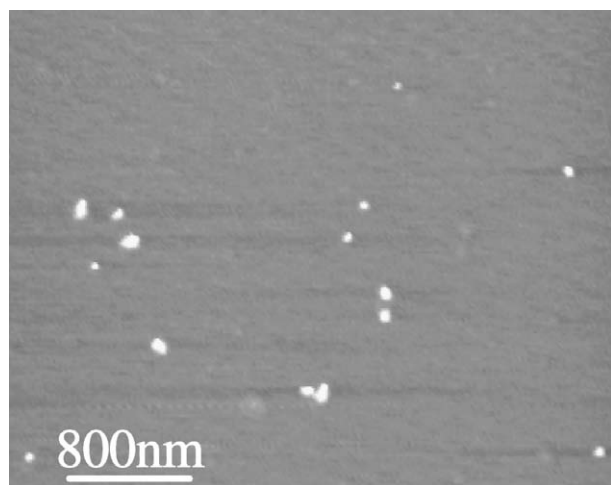


Figure 5. AFM image of dextran spray-dried on mica; polymer concentration 5 $\mu\text{g}/\text{mL}$.

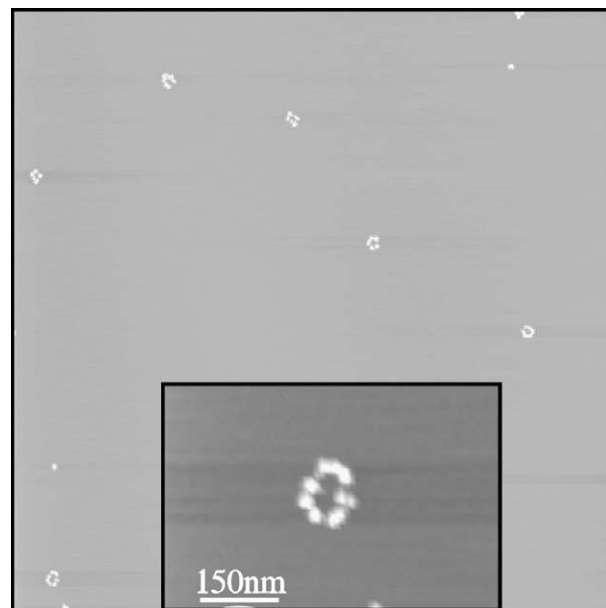


Figure 6. AFM image of the Ca^{2+} salt form of Mn A spray-dried on mica; polymer concentration 5 $\mu\text{g}/\text{mL}$. An enlargement of the object at the bottom left corner is shown in the inset.

different polymeric molecules resulting in aggregation. Unexpectedly, only a small number of spherical particles (6 to 7) participated in aggregation giving rise to a 'toroidal-like' structure. Thus, at the divalent ions concentration used in these experiments, the interaction with calcium ions seemed to preclude the formation of large aggregates, as indicated by the light scattering findings which did not show a continuous increase of the scattered light intensity. However, it cannot be excluded that different experimental conditions might lead to different morphologies.

The evaluation of the dimensions of the objects revealed by AFM imaging, and measured perpendicularly to the mica surface, confirmed the differences in the Mn A morphology for the different salt forms. The average thickness of the objects detected for the Mn A NH_4^+ form was 0.81 nm (standard deviation: 0.16 nm) in good agreement with the lateral dimension of a polysaccharide single chain.^{11,12} In contrast, the dimension of the spheres detected for the Na^+ form was 3.65 nm (standard deviation: 0.51 nm). The thickness of the single spheres in the aggregates imaged with the Ca^{2+} form was 3.99 nm (standard deviation: 0.60 nm).

In conclusion, the capsular polysaccharide produced by *N. meningitidis* group A exhibited conformational behavior dependent on the nature of its counterion. For the monovalent cations, the sodium form showed a spherical shape, whereas the NH_4^+ form resulted in a more elongated structure. The interaction with calcium ions produced 'toroidal' aggregates of spherical particles, which also explains the lower solubility of the polymer in the presence of calcium ions. The aggregates would also hinder access of the periodate ion to the available diols of the polysaccharide and thus account for its resistance to periodate oxidation.

1. Experimental

1.1. Preparation of polysaccharides samples and CaCl_2 solution

The capsular polysaccharide produced by *N. meningitidis* group A was received in the Ca^{2+} form. To convert it into the sodium or ammonium salt forms, it was dissolved in 100 mM sodium or ammonium phosphate buffers, respectively, to give a solution of

10 mg/mL concentration. In both cases, a precipitate constituted of calcium phosphate was formed and the suspensions were allowed to stand at 4 °C overnight to assure complete precipitation. The precipitates were removed by centrifugation and the supernatants were subjected to a colorimetric determination of total carbohydrates using the phenol–sulfuric acid test,¹³ which confirmed that polysaccharide was in the supernatants. The supernatants were then dialyzed at 4 °C against 0.1 M NaCl or NH₄Cl, followed by water. The pH of the solutions was adjusted to 7 by addition of 1 M NaOH or NH₄OH. The samples were recovered by lyophilization to give the polysaccharide in the Na⁺ (Mn A Na⁺) or NH₄⁺ salt form (Mn A NH₄⁺).

A solution of CaCl₂ in water was prepared and its concentration was determined via titration (Calcium-Test Aquamerck®, Merck) to be 92.16 mN. This solution was then diluted with 0.5 M NaCl in order to obtain a CaCl₂ solution 82.9 mN in 0.05 M NaCl, which was used for the experiments.

1.2. Light scattering experiments

Light scattering measurements were obtained at 25 °C with a Perkin–Elmer LS50B luminescence spectrometer, detecting the emitted radiation at 90°. Excitation and emission wavelengths were set at 600 nm (7.5 nm slit width). All solutions were filtered through 0.45-μm HA Millipore membrane before being used. Analyses were performed using a solution of Mn A Na⁺ 2 mg/mL in 0.05 M NaCl, corresponding to a concentration of 5.8×10^{-3} N (normality refers to concentration of polymer repeating units). Aliquots of the CaCl₂ solution 82.9 mN in 0.05 M NaCl were added to the Mn A Na⁺ solution maintaining the value of the ratio $R = [\text{Ca}^{2+}]/[\text{Mn A}]$ between 0 and 3.

1.3. Circular dichroism

Circular dichroism spectra were recorded with a Jasco J-600 instrument in the wavelength region from 190 to 260 nm at room temperature. A correction for the solvent baseline was made digitally in each case. All solutions were filtered through 0.45 μm HA Millipore membrane before being used. The analyses were performed using 10^{−4} N aqueous solutions of Mn A Na⁺ and Mn A NH₄⁺. Aliquots of the CaCl₂ solution 82.9 mN in 0.05 M NaCl were

added to the Mn A Na⁺ solution maintaining the value of the ratio $R = [\text{Ca}^{2+}]/[\text{Mn A}]$ between 0 and 3. The results were expressed as molar ellipticity at 200 nm ($[\theta]_{200 \text{ nm}}$).

1.4. Atomic force microscopy

AFM topography images were obtained with a Multimode Scanning Probe (Veeco) coupled with a Nanoscope IIIa control device. Tips, purchased from Veeco, were made of phosphorus-doped silicon. Aqueous solutions of Mn A Ca²⁺, Mn A Na⁺, Mn A NH₄⁺ and dextran at a concentration of 5 μg/mL were filtered with a 0.22 μm Millex® GP membrane (Millipore), before being spray-dried onto a freshly cleaved mica surface 15 h prior to imaging.

Acknowledgements

Professor M. Prato (University of Trieste, Italy) is kindly acknowledged for the use of the Atomic Force Microscope; the Regione Friuli Venezia Giulia (Projects # L.R.11/2003 and L.R.26/2005), the Italian Ministry of Foreign Affairs, and the South African National Research Foundation are acknowledged for funding; the Meningitis Vaccine Project is kindly acknowledged for providing the polysaccharide samples.

References

1. Trotter, C. L.; Greenwood, B. M. *Lancet Infect. Dis.* **2007**, *7*, 797–803.
2. LaForce, F. M.; Konde, K.; Viviani, S.; Préziosi, M. P. *Vaccine* **2007**, *25*, A97–A100.
3. Frasc, C. E. *Expert Opin. Biol. Ther.* **2005**, *5*, 273–280.
4. LaForce, F. M. *Abstracts of Papers*, 16th International Pathogenic Neisseria Conference (IPNC 2008), Rotterdam, The Netherlands, Sep 2006; O62.
5. Morris, E. R.; Rees, D. A.; Robinson, G. J. *Mol. Biol.* **1980**, *138*, 349–362.
6. Gacesa, P. *Carbohydr. Polym.* **1988**, *8*, 161–182.
7. Grasdalen, H.; Smidsrød, O. *Carbohydr. Polym.* **1987**, *7*, 371–393.
8. Korner, R.; Limberg, G.; Mikkelsen, J. D.; Roepstorff, P. *J. Mass Spectrom.* **1998**, *33*, 836–842.
9. Cescutti, P.; Rizzo, R. *J. Agric. Chem.* **2001**, *49*, 3262–3267.
10. Abu-Lail, N. I.; Camesano, T. A. *J. Microsc.* **2003**, *212*, 217–238.
11. Herasimenka, Y.; Cescutti, P.; Sampaio Noguera, C. E.; Ruggiero, J. R.; Urbani, R.; Impallomeni, G.; Zanetti, F.; Campidelli, S.; Prato, M.; Rizzo, R. *Carbohydr. Res.* **2008**, *343*, 81–89.
12. McIntire, T. M.; Brant, D. A. *Biopolymers* **1997**, *42*, 133–146.
13. Dubois, M.; Gilles, K. A.; Hamilton, J. K.; Rebers, P. A.; Smith, F. *Anal. Chem.* **1956**, *28*, 350–356.